Journal of Power Sources 196 (2011) 3962–3971

Contents lists available at ScienceDirect

Journal of Power Sources

journal homepage: www.elsevier.com/locate/jpowsour

Development and performance characterization of an electric ground vehicle with independently actuated in-wheel motors

Rongrong Wang, Yan Chen, Daiwei Feng, Xiaoyu Huang, Junmin Wang*

Department of Mechanical and Aerospace Engineering, 201 W. 19th Ave., The Ohio State University, Columbus, OH 43210, USA

ARTICLE INFO

Article history:
Received 5 October 2010
Received in revised form
29 November 2010
Accepted 29 November 2010
Available online 8 December 2010

Keywords:
Electric vehicles
In-wheel motors
Four-wheel independently actuated
Efficiency

ABSTRACT

This paper presents the development and experimental characterizations of a prototyping pure electric ground vehicle, which is equipped with four independently actuated in-wheel motors (FIAIWM) and is powered by a 72 V 200 Ah $LiFeYPO_4$ battery pack. Such an electric ground vehicle (EGV) employs four in-wheel (or hub) motors to independently drive/brake the four wheels and is one of the promising vehicle architectures primarily due to its actuation flexibility, energy efficiency, and performance potentials. Experimental data obtained from the EGV chassis dynamometer tests were employed to generate the in-wheel motor torque response and power efficiency maps in both driving and regenerative braking modes. A torque distribution method is proposed to show the potentials of optimizing the FIAIWM EGV operational energy efficiency by utilizing the actuation flexibility and the characterized in-wheel motor efficiency and torque response.

1. Introduction

Hybrid electric vehicles (HEV), plug-in hybrid electric vehicles (PHEV), and pure electric vehicles (EV) have been considered as promising vehicle architectures due to their potentials in emissions and fuel consumption reductions [1–3,11,12]. Among these vehicle architectures, electric vehicle with four independently actuated in-wheel motors (FIAIWM) is an emerging one with unique features. A FIAIWM electric vehicle employs four in-wheel (or hub) motors to directly actuate its four wheels, without any mechanical links, such as transmissions or differentials, among them. The torque as well as driving/braking mode of each wheel can be controlled independently. Such actuation flexibilities together with the electric motors' fast and precise torque responses not only can enhance vehicle motion/stability control performance [4,5,20] but also offer new avenues for improving the EGV operational energy efficiency.

There are several key features that clearly distinguish FIAIWM EGVs from other HEVs, PHEVs, and EVs particularly from the operational energy and power efficiency optimization perspective. In a typical HEV or PHEV configuration, a single high-speed motor is connected with the engine in series or in parallel to formulate a hybrid powertrain, whose power is transmitted to the ground wheels through mechanical drivetrains [1,6]. Such mechanical connections make the actuation mode (driving or braking) and torque among wheels coupled. Moreover, as speed reduction mechanisms (e.g. transmissions) are usually utilized between the hybrid powertrain and the wheels in HEVs and PHEVs, the desired motor characteristics are quite different from the ones for FIAIWM EGV's in-wheel motors which directly drive/brake wheels without gear reductions. Furthermore, as Fig. 1 illustrates, the in-wheel motors are part of the unsprung mass and will directly experience different and time-varying normal forces induced by static and dynamic load transfers during vehicle dynamic operations and maneuvers. A FIAIWM EGV possesses the ability of better utilizing the different normal forces by separately controlling the respective in-wheel motors at the vehicle corners. Such a capability however does not exist on HEVs and PHEVs where the wheels are actuated by a sprung and centralized powertrain.

The aforementioned unique features of FIAIWM electric vehicles suggest that detailed knowledge on torque response and energy efficiency characteristics of in-wheel motor and its driver, at both driving and regenerative braking modes, are necessary for further research on improving FIAIWM EVG operational energy efficiency and motion control performance. As an emerging vehicle architecture, FIAIWM EGV's performance and efficiency characterizations are rarely available in the open literature. Several ground vehicle performance analysis and power management studies have been previously reported in the literature [6–9]. However, most of those research work were for conventional or hybrid electric vehicle architectures, but not the FIAIWM EGVs. Power management methods for HEVs have been extensively investigated and the main foci are on the coordination of engine and motor usages, regenerative braking energy harvesting, battery management, and engine operations [6,8,10], but not at the torque distribution and opti-

* Corresponding author. Tel.: +1 614 247 7275; fax: +1 614 292 3163.
E-mail address: wang.1381@osu.edu (J. Wang).

0378-7753/$ – see front matter © 2010 Elsevier B.V. All rights reserved.
doi:10.1016/j.jpowsour.2010.11.160

Nomenclature

U	battery voltage
I	battery current
P	battery power
k	motor control gain
ω	wheel rotational speed in rad/s
T_i	torque provided by the ith in-wheel motor
T_{dr}	desired driving torque
T_{br}	desired braking torque
η_d	motor efficiency in driving mode
η_b	motor efficiency in braking mode

mization at the individual wheel level, which is needed for FIAIWM EGVs. Recently, research on vehicles with in-wheel motors has been active. In-wheel motor selection criteria for hybrid electric vehicle applications have been discussed in [13,14]. Different groups of researchers reported vehicle motion and stability control enhancement methods using in-wheel motors for unmanned and manned vehicle applications, without specific considerations on in-wheel motor torque responses and energy efficiency characterizations [5,15–17].

In this paper, experimental characterizations of an in-wheel motor and motor driver pair torque responses, power consumptions, and energy efficiencies at both driving and regenerative braking modes are conducted based on the experimental data obtained in chassis dynamometer tests of a prototyping FIAIWM EGV developed by Ohio State University. The characterizations reveal the in-wheel motor/driver torque response and energy efficiency with respect to wheel speed and control signal, and thus provide foundational information for FIAIWM EGV control and energy efficiency optimization. As the in-wheel motor/driver efficiency curves are not strictly concave or convex, a numerical solution is proposed to show the potentials of improving FIAIWM EGV operational energy efficiency by appropriately allocating the total required torque among the four in-wheel motors. To the authors' best knowledge, this paper first presents the detailed design, performance, and energy efficiency characterization results for FIAIWM electric ground vehicles in the open literature.

The rest of the paper is organized as follows. Description and experimental setup of a FIAIWM EGV are presented in Section 2. FIAIWM EGV performance and energy efficiency characterizations using chassis dynamometer test data are described in Section 3. The FIAIWM EGV energy efficiency analyses are provided in Section 4. A torque allocation method to improve the FIAIWM EGV operational energy efficiency is shown in Section 5 followed by conclusive remarks.

Table 1
Parameters of the EGV and main components.

Parameters	Values
EGV parameters	
Total mass	800 kg
Wheel base	1.89 m
Maximal speed	100 km h^{-1}
Hub motor and tire parameters	
Motor mass	25 kg
Combined inertia of motor, wheel, and tire	2.31 kg m^2
Tire effective radius	0.33 m
Maximal motor power	7.5 kW
Maximal motor torque	150 N m
Maximal motor rotational speed	900RPM
Battery parameters	
Number of battery cells	22
Battery pack voltage	72 V
Nominal capacity	200 Ah
Maximal current	800 A
Battery cell mass	3.6 kg
Cell dimension	0.36 m × 0.065 m × 0.28 m

2. FIAIWM EGV description and experimental setup

2.1. FIAIWM EGV description

Fig. 1 shows the developed prototyping FIAIWM EGV and the in-wheel motors. Each wheel is independently actuated by a customized 7.5Kw in-wheel motor which is mounted in the wheel. Due to the requirements on power density, compactness, light weight, as well as cost, permanent-magnet brushless direct-current (BLDC) electric motors were chosen to make the in-wheel motors [18]. The key parameters of the FIAIWM EGV and the main components are listed in Table 1.

The driving/braking mode and torque of each wheel can be controlled independently by giving different control signals to the respective motor driver, which contains power electronics adjusting the three-phase currents to the BLDC motor according to the control signal. The rotational speed of each wheel is precisely measured by an active speed sensor and a tooth-wheel mounted on the motor as shown in Fig. 1. In the motor driving or regenerative braking mode, the motor control voltage signal, Cv, to the motor driver ranges from 1 V to 3.4 V, corresponding to zero to maximal (driving or regenerative braking) torque values.

The only power source of the EGV is a 72 V lithium-ion power battery pack which is composited by 22 battery cells connected in series, as shown in Fig. 2. The battery pack has a 200 Ah nominal capacity and can deliver a peak power of 40 kW. Each battery cell is equipped with a battery management system (BMS) chip which can monitor the battery states such as battery voltage, state of charge (SOC), and state of healthy (SOH). The BMS can also automatically balance the battery voltages based on the measured voltage differences among the battery cells.

Fig. 1. EGV and the installed in-wheel motors.

Fig. 2. Li-ion batteries installed on the FIAIWM EGV.

All the electrical components on the EGV are powered by the battery pack through DC/DC converters or DC/AC inventers. A 72–12 V DC/DC converter is utilized for powering a dSPACE real-time prototyping controller and the BMS. A 12–5 V DC/DC converter provides power to the EGV sensors. Also, a 12–110 V DC/AC inverter is used to power a laptop on the EGV. The main circuit are protected by a key switch which controls the on/off of a main relay. Four manual switches are used to control the connection/disconnection of the driver/motor pairs individually for safety reasons. Fig. 3 illustrates the electric circuit diagram of the prototyping FIAIWM EGV.

2.2. Experimental system setup

The FIAIWM EGV tests were conducted on a twin-roll chassis dynamometer as shown in Fig. 4. The in-wheel motor torque values at different speeds and torque control signals were measured by a torque sensor equipped on the chassis dynamometer. The chassis dynamometer roller frictional torque and EGV wheel frictional torque were carefully calibrated at different speeds before conducting the EGV tests. All of these frictional torque losses are considered in the EGV performance data analyses presented in the later sections. The EGV battery voltage and current were measured by a voltage sensor and a current sensor to calculate the motor efficiency and power. In the in-wheel motor and battery performance tests, the motor control signals were changed from 1.0 V to 3.0 V with a 0.2 V step at different motor speeds. The parameters in Table 1 and an air drag coefficient of 0.5 were used for the chassis dynamometer controller to simulate the EGV real road resistance. A dSPACE MicroAutoBox was used to control and record all the EGV and chassis dynamometer signals in real-time.

3. EGV performance and energy efficiency characterizations

In this experimental characterization, the in-wheel motor and its respective motor driver are treated as a unit. The input of the motor/motor driver pair is the torque control signal and the output is the measured motor torque. The motor driver was set in the torque mode, which means that the motor driver will make the motor deliver a certain torque value with respect to a control signal voltage. In the driving mode, the in-wheel motors convert the battery power to driving torque. The measured motor driving torque at different speeds and control inputs are shown in Fig. 5,

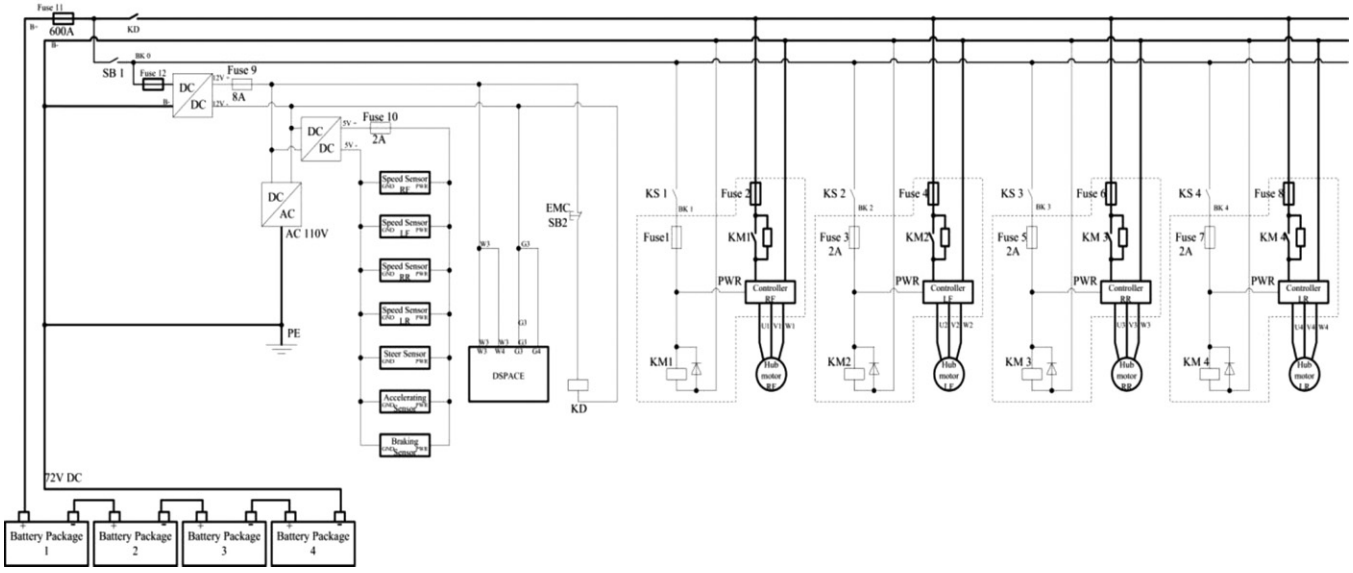

Fig. 3. Electric circuit diagram of the prototyping FIAIWM EGV.

Fig. 4. FIAIWM EGV chassis dynamometer test setup.

which indicates that the motor torque is proportional to the control input at different speeds. Therefore, one can define the motor torque control gain as

$$k = \frac{\text{motor torque}}{\text{motor control signal}}, \quad (1)$$

which is nearly constant across the entire speed range as Fig. 5 shows. Note that some motor torque values are lower around 450RPM in comparison to the torque levels at neighboring speeds. This may be attributed to the temperature control function of the motor driver which will actively reduce the current delivered to the motor (causing torque reduction) if it detects that the motor/driver temperature is higher than a certain safety threshold during the chassis dynamometer tests due to the lack of cooling. Such an explanation can also be supported by the smoothness of the torque/current ratio surface as shown in Fig. 9 later. In actual EGV road operations, the probability of this over-temperature case will be very low thanks to the sufficient air-cooling effects. Despite this small valley on the motor torque response surface, the control gain can still be approximated as a constant. In fact, during our field tests of the FIAIWM EGV, motor over-temperature case never happened.

The motor power is also plotted in Fig. 5, with the maximal power being close to 7.5 kW at high speeds. Fig. 6 shows the measured battery voltage and current.

When the in-wheel motor works in regenerative braking mode, it actually acts as a generator and converts the kinetic energy of EGV to electricity and charges the batteries. For the in-wheel motor regenerative braking tests, the measured motor torque and power at different control signals and speeds are shown in Fig. 7. Similar to the driving mode, control gains at different speeds are almost the same except at the very low speeds. The maximal regenerative braking torque of a single in-wheel motor is around 80 Nm, which means that the regenerative braking torque from the four motors together can make the EGV reach a maximum deceleration of 1.2 m/s^2. Fig. 7 also shows that the motor regenerative braking torque is almost zero when motor speed is less than 200RPM, where the motor cannot generate sufficient electricity. It is interesting to note that the in-wheel motor/driver regenerative braking torque surface is smooth without valleys. This smoothness is largely because that the motor/driver temperature was low at regenerative braking mode and the motor driver's temperature limiting function was not triggered.

The measured battery current and voltage during the regenerative braking tests are shown in Fig. 8. As expected, the charging current from the in-wheel motor increases with the increasing motor control signal and speed.

For BLDC motors, the equivalent current delivered to the motor driver is proportional to the motor torque [17,18]. The ratio defined as motor torque/battery current (consumed or generated) at different speeds and control signals during both driving and regenerative braking modes are shown in Fig. 9. This ratio becomes smaller with the increasing motor speed at both driving and regenerative braking modes. The smoothness of the surfaces also supports the explanation (current limiting) for the small valley occurred on the driving torque surface plotted in Fig. 5.

The preceding in-wheel motor/driver driving and regenerative braking torque response characteristics are important for FIAIWM EGV road operations. For example, for conventional vehicles, HEVs, and PHEVs, mechanical differentials are equipped to connect the driving wheels and to allow different rotational speeds for the inner and outer wheels when turning corners. For FIAIWM EGVs, there is not a differential connecting the wheels and thus the wheel torques and speeds have to be precisely controlled to meet the vehicle driving and motion control requirements. The almost speed-independent and linear relationship between control signal and motor driving/braking torque thus make the precise wheel torque and speed control possible, without wheel torque measurement which may not be available on vehicles.

A chassis dynamometer simulated road test was also carried out to show the vehicle acceleration and deceleration performance purely by the in-wheel motors. In the simulated road test, identical control signals were given to the two front wheels, placed on the twin rollers of the chassis dynamometer, for driving/braking the EGV. The vehicle speed and in-wheel motor control signal are plotted in Fig. 10 while the battery current and voltage are shown in

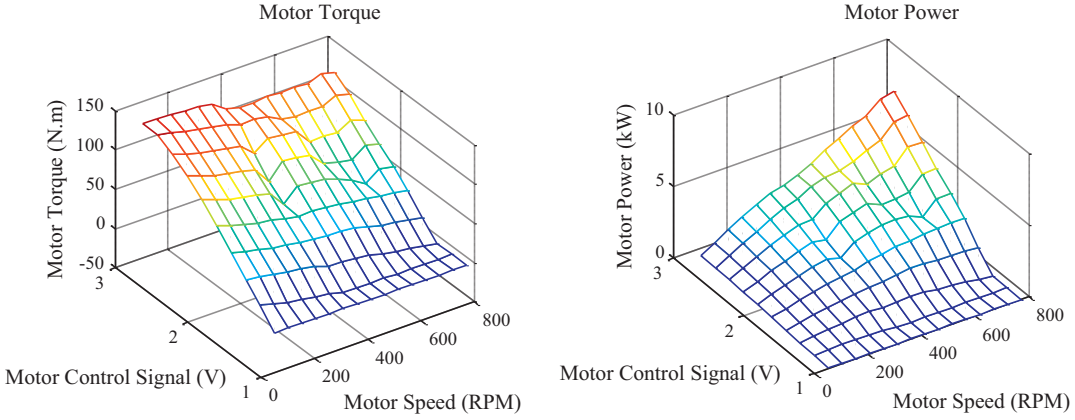

Fig. 5. Motor torque and power at different speeds and motor torque control signals in driving mode.

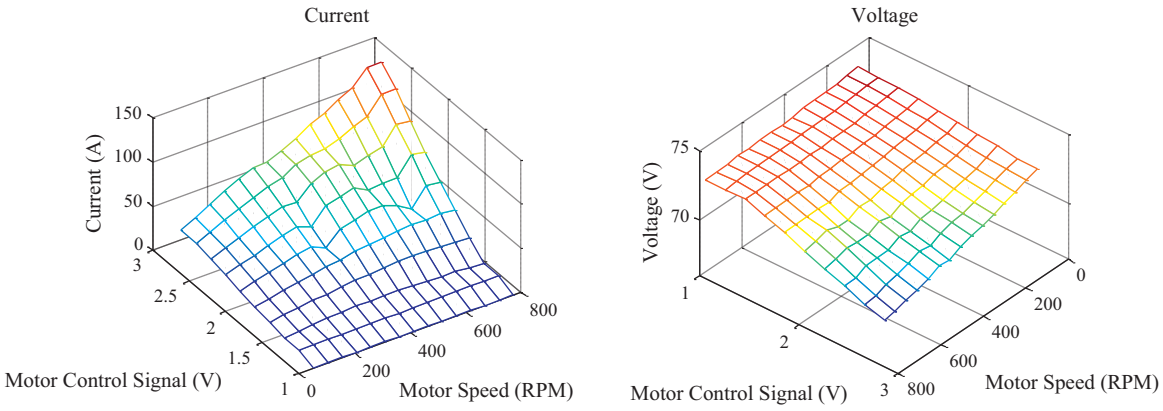

Fig. 6. Battery current and voltage at different motor torque control signals and motor speeds.

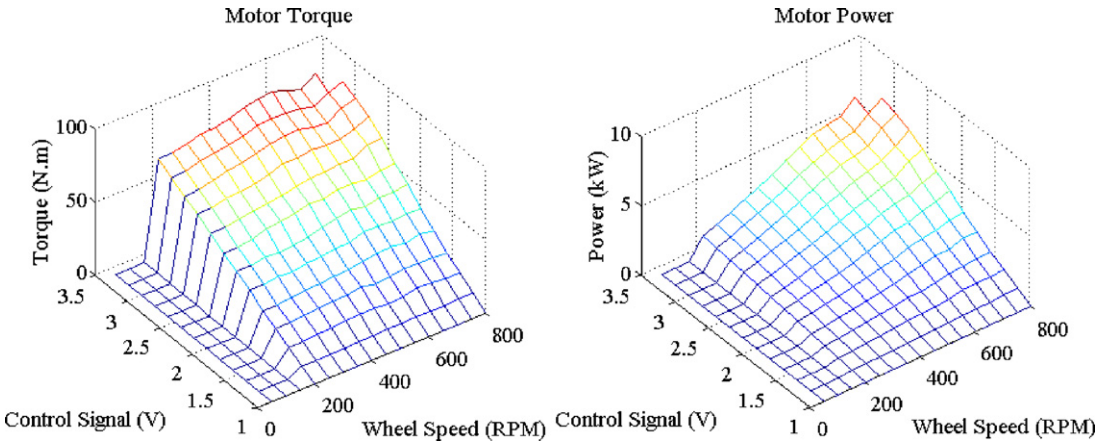

Fig. 7. In-wheel motor regenerative braking torque and power.

Fig. 11. The positive control signal means the motors were in driving mode while the negative control signal indicates that the motors were performing regenerative braking. As the two figures indicate, the positive and negative motor control signals could make the vehicle accelerate and decelerate, respectively. The EGV acceleration/deceleration was also proportional to the absolute values of the control signal. Correspondingly, as Fig. 11 shows, when the motor control signal was negative, the battery current was also negative, meaning that the batteries were being charged when the EGV was decelerating due to the regenerative braking of the in-wheel motors. One can also note that in Fig. 11, the battery current absolute value goes larger with the increase of vehicle speed even if the control signal does not change. This trend is because more battery power is needed or generated by the motors at high speeds and this observation matches with the in-wheel motor/driver test results presented in Fig. 9.

4. FIAIWM EGV energy efficiency analyses

Energy efficiency is very important for electric vehicles to optimize their operational energy consumptions and to maximize their travel ranges. There are two kinds of efficiencies that can be studied

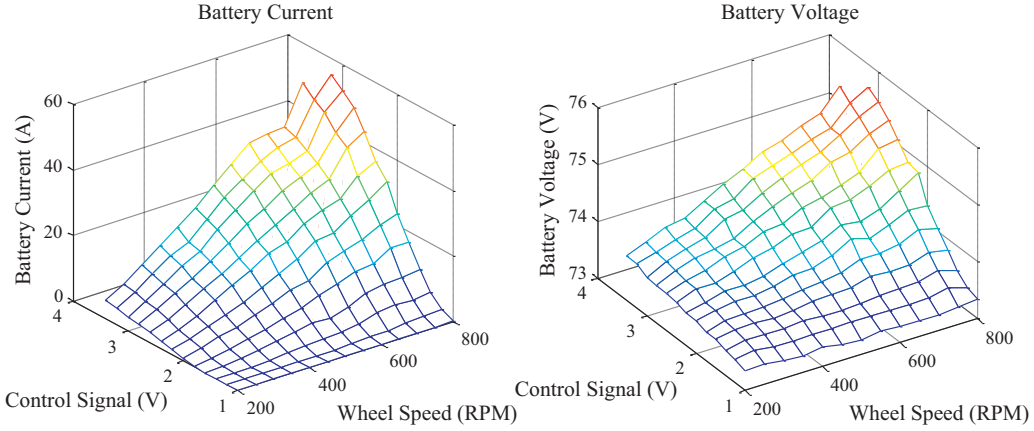

Fig. 8. Battery current and voltage in the regenerative braking tests.

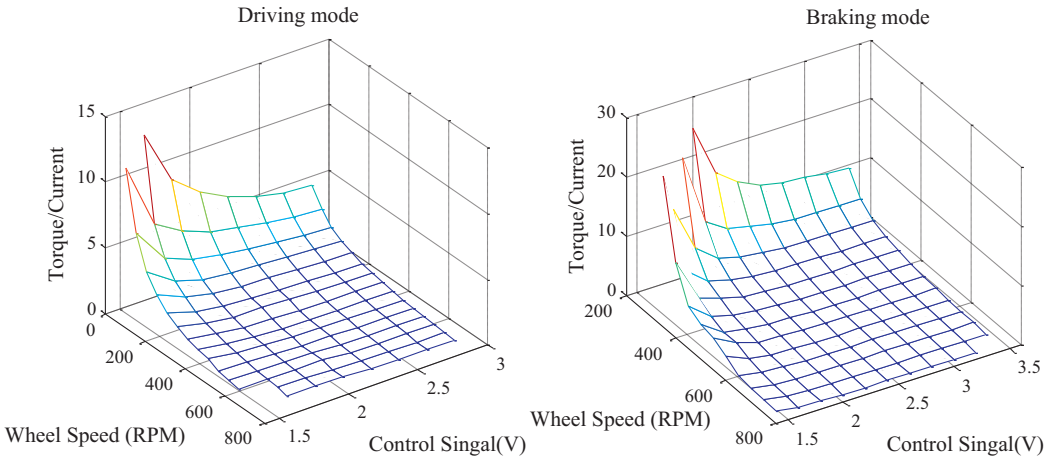

Fig. 9. Motor torque/battery current at different speeds and loads.

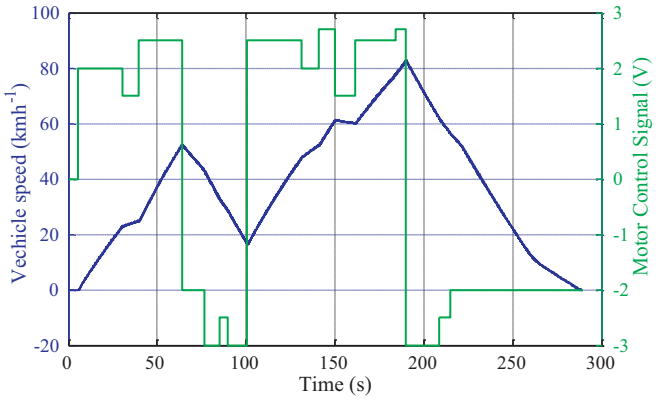

Fig. 10. Vehicle speed and in-wheel motor control signals during the simulated road test on a chassis dynamometer.

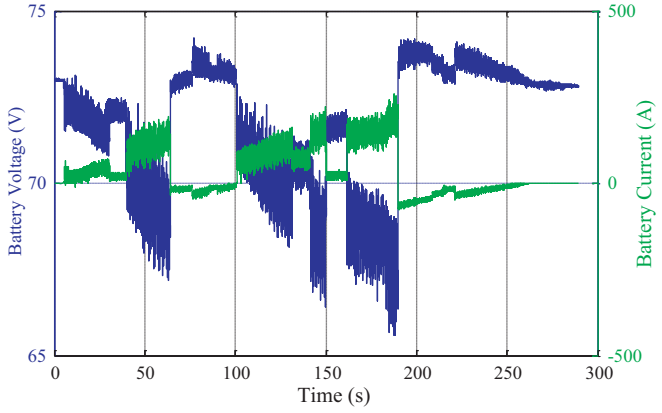

Fig. 11. Battery current and voltage during the simulated road test on a chassis dynamometer.

for the driving case. One is the battery to in-wheel motor efficiency, which describes how much battery power is transferred to the motor output power and is mostly determined by the in-wheel motor/driver performance, and can be defined as

$$\text{Battery-to-motor efficiency} = \frac{\text{motor power}}{\text{battery power}} \quad (2)$$

The other efficiency is the battery-to-ground efficiency. Unlike the battery-to-motor efficiency, the battery-to-ground efficiency considers the losses due to wheel friction and tire rolling resistance, this efficiency is defined as:

$$\text{Battery-to-ground efficiency} = \frac{\text{motor power} - \text{power losses}}{\text{battery power}} \quad (3)$$

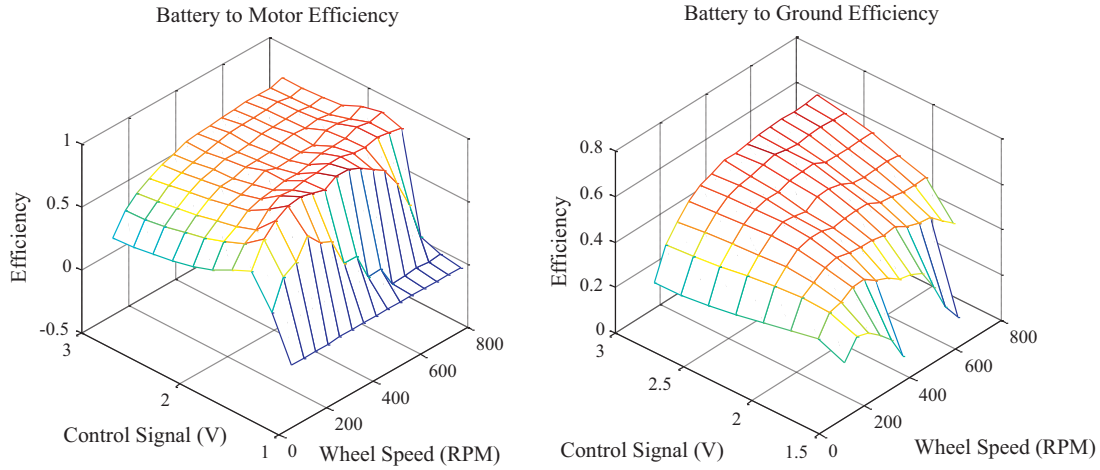

Fig. 12. Battery-to-motor and battery-to-ground efficiencies at different motor torque levels and speeds in driving mode.

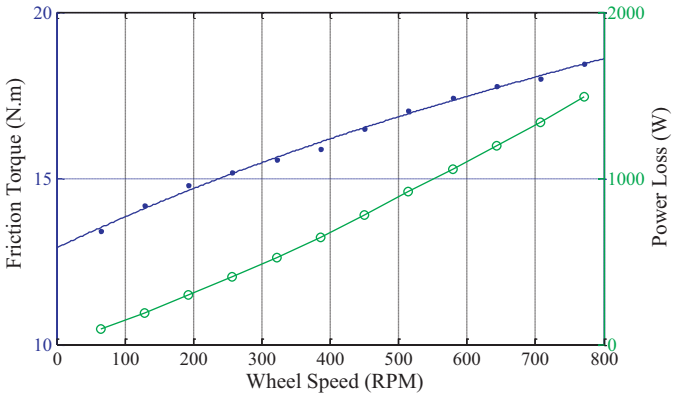

Fig. 13. Power losses caused by the motor friction and tire rolling resistance.

The battery-to-ground efficiency is also important in the EGV power management design, as it includes the parasitical loss characteristics. These two kinds of efficiencies at different in-wheel motor control signals and speeds are plotted in Fig. 12. Note that for the battery-to-motor efficiency map, some negative values appeared at low torque regions. This may be caused by the torque measurement inaccuracy (low signal to noise ratio) at low torque levels.

Fig. 12 shows that the battery-to-motor efficiency becomes higher at high motor speeds. Moreover, at a given speed, the battery-to-motor efficiency increases with the increasing motor control signal before it reaches the maximal efficiency, and then it slowly decreases to a constant value. The battery-to-ground efficiency is always lower than the battery-to-motor efficiency due to the wheel power losses, which are shown in Fig. 13. Fig. 12 also illustrates that the battery-to-ground efficiency almost drops to 0 if the motor control signal is smaller than 1.5 V. This indicates that the motor torque will be smaller than the wheel frictional torque if the control signal is less than 1.5 V.

Similar to the efficiency definitions in the driving mode, the motor regenerative braking efficiencies can also be divided into motor-to-battery efficiency and ground-to-battery efficiency. The ground-to-battery efficiency describes how much power generated by tire force can be converted into battery power. It can be defined as

$$\text{Ground-to-battery efficiency} = \frac{\text{battery power}}{\text{tire force} \times \text{wheel speed}} \tag{4}$$

or

$$\text{Ground-to-battery efficiency} = \frac{\text{battery power}}{\text{motor torque} \times \text{motor speed} + \text{power losses}} \tag{5}$$

The motor-to-battery efficiency does not consider the frictional loss of the wheel or rolling resistance, and thus is determined by only the motor and motor driver performance. The motor-to-battery efficiency is defined as:

$$\text{Motor-to-battery efficiency} = \frac{\text{battery power}}{\text{motor torque} \times \text{motor speed}} \tag{6}$$

The two efficiencies in the regenerative braking mode are shown in Fig. 14, which indicates that motor-to-battery efficiency is always higher than the ground-to-battery efficiency due to the power losses. Fig. 14 also indicates that both efficiencies increase with the increase of wheel speed and motor control signal.

5. Discussions on FIAIWM EGV energy optimization

As there are four in-wheel motors independently actuating the four wheels of FIAIWM EGV, this actuation flexibility can be possibly utilized for improving the EGV operational efficiency by allocating different torques to the four wheels with respect to the desired total torque and motor/driver efficiency. This section discusses on the FIAIWM EGV energy optimization issues and tries to show the energy efficiency improvement potentials enabled by the FIAIWM. As the in-wheel motor/driver efficiency curves are not strictly concave or convex, it is challenging to get an analytic solution on how to allocate the desired total torque to the four in-wheel motors for achieving the highest EGV energy efficiency. Here, a simple numerical method is proposed for illustrating the potentials on improving FIAIWM EGV operational energy efficiency, which is a challenging and involved research topic that deserves further in-depth studies.

5.1. Energy optimization in driving

The objective is to minimize the power consumed by the four motor/motor driver pairs as expressed by

$$P = U(I_{fl} + I_{fr} + I_{rl} + I_{rr}), \tag{7}$$

where U is the battery voltage. According to the driving efficiency definition, the in-wheel motor efficiency in driving mode can be written as

$$\eta_{di} = \frac{\omega T_i}{UI_i}, \tag{8}$$

where $i \in Q := \{fl\, fr\, rl\, rr\}$ indicates the specific wheel, ω is the wheel/motor speed in rad/s, I_i is battery current that each motor consumes, T_i is the motor torque. Thus, battery power consumed by each wheel can be written as

$$P_i = UI_i = \frac{\omega \times T_i}{\eta_d}. \tag{9}$$

Note that the efficiency η_d is a function of motor speed and torque. The in-wheel motor/driver efficiencies at driving and regenerative braking modes can be fitted as functions of motor torque and speed with experimental data as shown in Fig. 15.

The four torque values provided by the four in-wheel motors should satisfy the following equation for vehicle motion control purpose [4,19]:

$$\begin{cases} T_{rl} + T_{rr} + T_{fl} + T_{fr} = T_x \\ T_{rl} - T_{rr} + T_{fl} - T_{fr} = T_\Omega \end{cases}, \tag{10}$$

where T_x is the total torque generated by the motors to control the EGV longitudinal speed, and T_Ω is the torque split to control the EGV yaw rate. Base on the above equation, one has

$$\begin{cases} T_{rl} + T_{fl} = T_{dl} = \dfrac{T_x + T_\Omega}{2} \\ T_{rr} + T_{fr} = T_{dr} = \dfrac{T_x - T_\Omega}{2} \end{cases}, \tag{11}$$

where T_{dl} and T_{dr} indicate the desired total torque values for the two motors on the EGV's left and right sides, respectively. As the total torque of the two motors in the left or right side of EGV is known, so the energy optimization problem can be studied in half part of the vehicle.

Considering the right part of the vehicle, the energy optimization problem can be written as

$$\min(P_{fr} + P_{rr}), \text{ Subject to } T_{fr} + T_{rr} = T_{dr}. \tag{12}$$

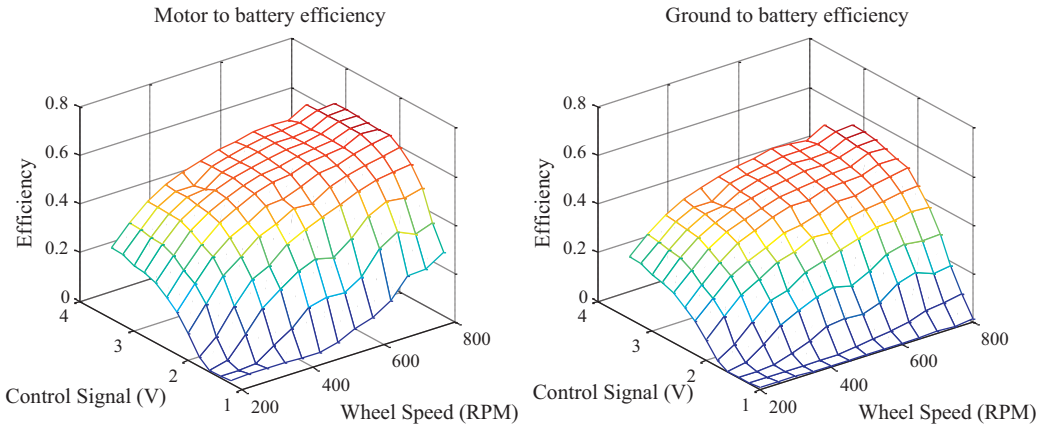

Fig. 14. Efficiencies in regenerative braking mode.

Thus, at a given speed, the battery power consumed by these two right-side motors can be written as

$$P_r = P_{fr} + P_{rr} = \frac{\omega \times T_{fr}}{\eta_d(T_{fr})} + \frac{\omega \times T_{rr}}{\eta_d(T_{rr})} \tag{13}$$

The next step is to choose a set of T_{fr}^* and T_{rr}^* which can minimize P_r. Rewrite the above equation as

$$P_r = \frac{\omega((T_{dr}/2) - \Delta T_r)}{\eta_d((T_{dr}/2) - \Delta T_r)} + \frac{\omega((T_{dr}/2) - \Delta T_r)}{\eta_d((T_{dr}/2) - \Delta T_r)}. \tag{14}$$

Note the T_{d_max} is the maximal driving torque a motor can provide. So ΔT_r should be bounded by

$$\begin{cases} \dfrac{T_{dr}}{2} - T_{d\_max} \le \Delta T_r \le T_{d\_max} - \dfrac{T_{dr}}{2} \\ -\dfrac{T_{dr}}{2} \le \Delta T_r \le \dfrac{T_{dr}}{2} \end{cases} \tag{15}$$

to make sure that the reference torque for a certain wheel is bounded between 0 and T_{d_max}. As the function $\eta_d(T)$ is known at a certain speed, the optimal value T_r^* can be found to minimize P_r. Since the two motors are assumed to be identical, there will be two ΔT^* that can achieve the optimal value of P_r. These two ΔT^* values will have the same absolute value but different signs. Note that in practical applications, the ΔT^* may not need to be solved on-line. Instead, ΔT^* may be obtained from a table $\Delta T^*(T_d,\omega)$ which can be generated off-line based on the experimental data. Once the ΔT^* is obtained, the torques for the right-side motors can be written as

$$\begin{cases} T_{fr}^* = \dfrac{T_{dr}}{2} \pm \Delta T_r^* \\ T_{rr}^* = \dfrac{T_{dr}}{2} \mp \Delta T_r^* \end{cases}. \tag{16}$$

Similarly, the optimal torques the left-side in-wheel motors can also be written as

$$\begin{cases} T_{fl}^* = \dfrac{T_{dl}}{2} \pm \Delta T_l^* \\ T_{rl}^* = \dfrac{T_{dl}}{2} \mp \Delta T_l^* \end{cases}. \tag{17}$$

Fig. 16 shows the optimized battery power consumed by the two right-side motors at different required torque levels. To better show the effectiveness of the proposed torque distribution method, the power consumption in the case of equally distributed torque mode and the case of two (only front or rear) wheels driving mode were also compared. It can be seen that the power consumption under the proposed torque distribution is always smaller than those of the other two cases. When the required torque is low, the optimized battery power is equal to that of the two-wheel-driving mode. The physical meaning is that the at small torque levels, the motor efficiency is low and only the front two or rear two motors are actuated to provide the required torque such that these two actuated motors can work at a higher efficiency range.

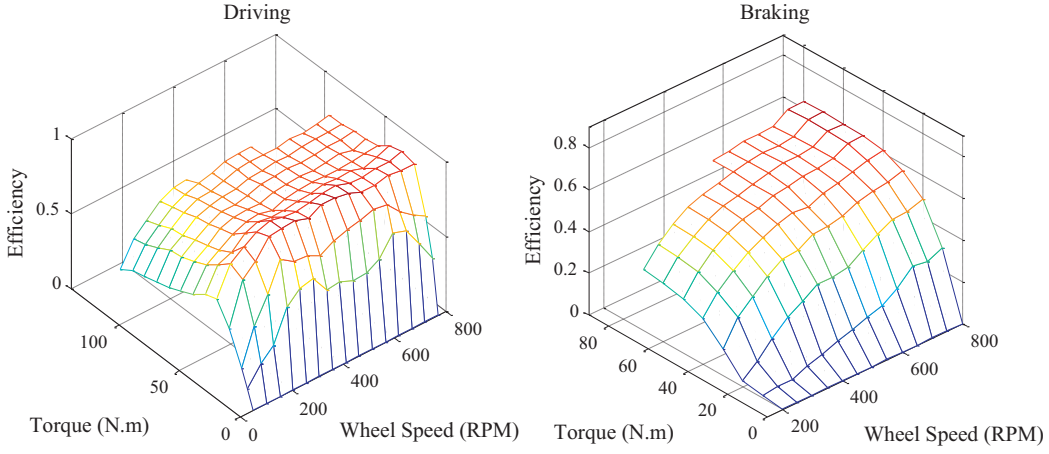

Fig. 15. Efficiencies as functions of in-wheel motor torques and speeds at driving and regenerative braking modes.

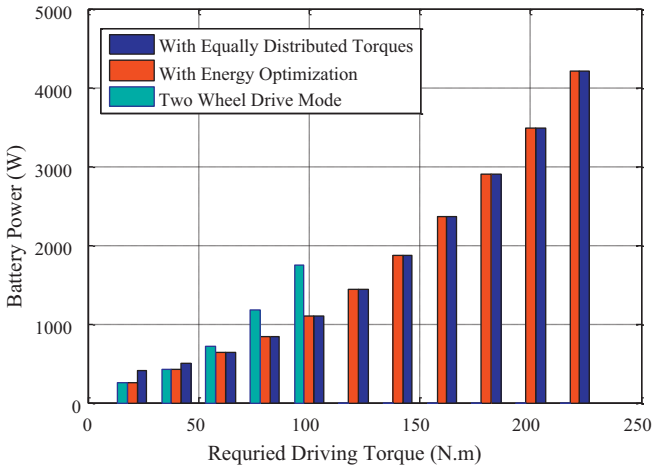

Fig. 16. Power consumption comparison in different driving torque distribution modes.

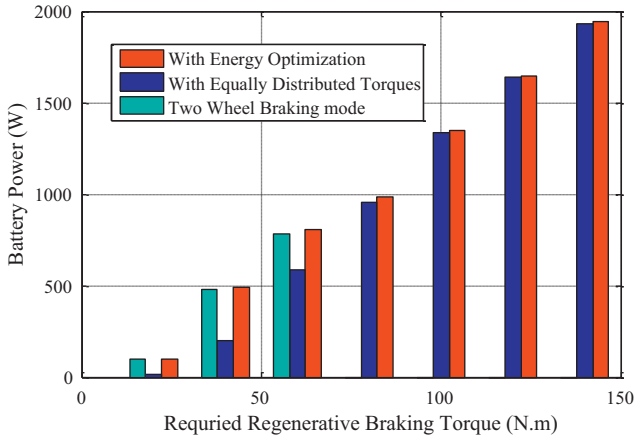

Fig. 17. Regenerative power comparison with different braking torque distribution methods (motor speed: 350RPM).

5.2. Energy optimization in regenerative braking

In the driving mode, the battery power should be minimized to reduce the power consumption. However, in the regenerative braking mode, the total power of the battery should be maximized to regenerate as much power as possible from the in-wheel motors at a given braking torque. Suppose that the desired total braking torque is not greater than the maximal braking torque that the four in-wheel motors can provide, the optimization problem in regenerative braking mode is to maximize the battery power defined in (7). Similar to the driving mode, the optimization problem in the regenerative braking mode can still be studied in half part of the vehicle. Considering the right side of the vehicle, the energy optimization problem in regenerative braking can be rewritten as

$$\max(P_{fr} + P_{rr}), \text{ with } T_{fr} + T_{rr} = \frac{T_{br}}{2}, \tag{18}$$

where T_{br} is the desired total braking torque the two right-side motors should provide.

According to the driving efficiency definition, the regenerative braking efficiency η_{bi} can be written as

$$\eta_{bi} = \frac{UI_i}{\omega T_i}. \tag{19}$$

The efficiency function $\eta_b(T)$ is fitted based on experimental data and is shown in Fig. 15. Thus, the power that the battery pack receives from each of the motors can be written as

$$P_i = \eta_{bi}\omega T_i \tag{20}$$

The power sent to battery from the two right-side motors can be written as

$$P_r = P_{fr} + P_{rr} = \omega \times \eta_{fr}(T_{fr}) \times T_{fr} + \omega \times \eta_{rr}(T_{rr}) \times T_{rr}. \tag{21}$$

Rewrite the above equation as

$$P_r = \omega\left(\frac{T_{br}}{2} - \Delta T_r\right) \times \eta_b\left(\frac{T_{br}}{2} - \Delta T_r\right) + \omega\left(\frac{T_{br}}{2} + \Delta T_r\right) \times \eta_b\left(\frac{T_{br}}{2} + \Delta T_r\right). \tag{22}$$

In order to constrain the braking torque from a motor within 0 and its maximal braking torque, $T_{b\text{-}max}$, ΔT_r should be bounded as

$$\begin{cases} \dfrac{T_{br}}{2} - T_{b-\max} \le \Delta T_r \le T_{b-\max} - \dfrac{T_{br}}{2} \\ -\dfrac{T_{br}}{2} \le \Delta T_r \le \dfrac{T_{br}}{2} \end{cases} \tag{23}$$

Thus the optimal value ΔT_r^* can be found to maximize the P_r. The optimized torque for each of the two right-side motors is shown as

$$\begin{cases} T_{fr}^* = \dfrac{T_{br}}{2} \pm \Delta T_r^* \\ T_{rr}^* = \dfrac{T_{br}}{2} \mp \Delta T_r^* \end{cases} \tag{24}$$

The optimal torques for the two left-side motors can also be similarly written as

$$\begin{cases} T_{fl}^* = \dfrac{T_{bl}}{2} \pm \Delta T_l^* \\ T_{rl}^* = \dfrac{T_{bl}}{2} \mp \Delta T_l^* \end{cases} \tag{25}$$

Fig. 17 shows the battery power in different regenerative braking torque distribution ways. As it indicates, the battery power with the proposed braking torque distribution is always greater than the ones by other braking torque distribution methods.

The preceding results show that by appropriately utilizing the actuation flexibility of the FIAIWM EGV and distributing the torque among the four in-wheel motors with respect to their energy efficiency characteristics, the battery power in the driving and regenerative braking modes can be either reduced or increased in comparison with the cases of equally distributed torque. Such an observation suggests that there are good potentials for improving the overall FIAIWM EGV operational energy efficiencies by allocating the total desired torque among the four in-wheel motors in an optimal way with respect to their different efficiencies and operating conditions.

6. Conclusions

In this paper, the experimental performance and energy efficiency characterizations of an electrical ground vehicle with four independently actuated in-wheel motors are presented. The torque responses and energy efficiencies of in-wheel motor/driver were intensively studied through experiments conducted on a chassis dynamometer with a prototyping FIAIWM EGV at both driving and regenerative braking modes. An in-wheel motor torque distribution method for improving the EGV operational energy efficiency was proposed based on the system and component efficiency characteristics, and the results show that there are good potentials for improving the overall FIAIWM EGV operational energy efficiencies by explicitly considering the in-wheel motor efficiency and operating conditions.

Acknowledgements

This research is supported by Office of Naval Research (ONR) Young Investigator Award No. N00014-09-1-1018, Honda-OSU Partnership Program, and OSU Transportation Research Endowment Program.

References

[1] C.C. Chan, Proc. IEEE (90) (2002) 245–247.
[2] S. Campanari, G. Manzolini, F.G. Iglesia, J. Power Sources 186 (2009) 464–477.
[3] G.J. Offer, D. Howey, M. Contestabile, R. Clague, N.P. Brandon, Energy Policy 38 (2010) 24–29.
[4] A Goodarzi, E. Esmailzadeh, IEEE/ASME Trans. Mech. 12 (6) (2007) 632–639.
[5] R. Wang, J. Wang, Proceedings of the 2010 ASME Dynamic Systems and Control Conference, 2010.
[6] P. Pisu, G. Rizzoni, IEEE Trans. Control Syst. Technol. 15 (May (3)) (2007) 506–518.
[7] J.R. Wagner, D.M. Dawson, Z. Liu, IEEE Trans. Vehicular Technol. 53 (1) (2003) 184–195.
[8] X Wei, L. Guzzella, V.I. Utkin, G. Rizzoni, J. Dyn. Syst. Measure. Control 129 (1) (2007) 13–19.
[9] O. Barbarisi, F. Vasca, L. Glielmo, Control Eng. Pract. 14 (2006) 267–275.
[10] L.V. Perez, G.R. Bossio, D. Moitre, G.O. Garcia, Math. Comput. Simul. 73 (2006) 244–254.
[11] Y. Wu, H. Gao, IEEE Trans. Vehicular Technol. 55 (6) (2006) 1748–1754.
[12] J.V. Mierlo, P.V. Bossche, G. Maggetto, J. Power Sources 128 (1) (2004) 76–89.
[13] J. Willberger, A. Rojas, H. Niederkofler, Energy efficiency and potentials of electric motor types for wheel hub applications, SAE Paper 2009-24-0158, 2009.
[14] J. Willberger, M. Ackerl, A. Rojas, H. Niederkofler, Motor selection criteria and potentials of electrified all wheel drive concepts for passenger cars by add-on wheel hub motors on the rear axle, SAE Paper 2010-01-1307, 2010.
[15] G. Bayar, A.B. Koku, E. Konukseven, Proceedings of the International Workshop on Unmanned Vehicles, Turkey, 2010, pp. 117–124.
[16] S. Sakai, H. Sado, Y. Hori, IEEE/ASME Trans. Mach. 4 (1) (1999) 9–16.
[17] Y. Hori, IEEE Trans. Ind. Electron. 51 (5) (2004) 954–962.
[18] K.T. Chau, C.C. Chan, C. Liu, IEEE Trans. Ind. Electron. 55 (6) (2008) 2246–2257.
[19] D. Kim, S. Hwang, H. Kim, IEEE Trans. Vehicular Technol. 57 (2) (2008) 727–735.
[20] J. Wang, R. Longoria, IEEE Trans. Control Systems Technol. 17 (3) (2009) 723–732.